

Bond-slip effect in steel-concrete composite flexural members: Part 2 – Improvement of shear stud spacing in SCP

WonHo Lee^a, Hyo-Gyoung Kwak^{*} and Joung Rae Kim^b

Department of Civil and Environmental Engineering, Korea Advanced Institute of Science and Technology,
291 Daehak-ro, Yuseong-gu, Daejeon 34141, Republic of Korea

(Received March 7, 2019, Revised July 13, 2019, Accepted August 22, 2019)

Abstract. The use of shear studs usually placed in the form of mechanical shear connectors makes it possible to adopt composite steel-concrete structures in various structures, and steel-concrete plate composite (SCP) is being seriously considered for the installation of storage tanks exposed to harsh environments. However, manufacturing of SCP must be based on the application of existing design guidelines which require very close arrangement of shear studs. This means that the direct application of current design guidelines usually produces very conservative results and close arrangement of shear studs precludes pouring concrete within exterior steel faceplates. In this light, an improved guideline to determine the stud spacing should be introduced, and this paper proposes an improved ratio of the stud spacing to the thickness of steel plate on the basis of numerous parametric studies to evaluate the relative influence of the stud spacing on the stability of the SCP.

Keywords: steel-concrete plate composite; shear stud spacing; local buckling; design guideline

1. Introduction

Steel-Concrete Plate composite (SCP) is a modularized construction member that saves construction time and cost. Since a modularized structure made of SCP does not require formworks or curing of concrete at the construction site, it can be constructed regardless of climate or locational conditions. Therefore, applying SCP to tank structures such as the containment structures of nuclear power plants and LNG storage tanks installed in harsh environments has been widely considered. SCP consists of a concrete block with two steel plates attached at both sides of the concrete matrix and connected by studs, and the studs are welded to a steel plate and embedded into the concrete. Accordingly, it is important for the studs to resist shear stress and to prevent separation between concrete and the steel plate. In particular, SCP develops structural instability due to the yielding or local buckling of steel plates when it is subjected to large external loads, and thus the determination of stud spacing and thickness of steel plate has been the main issue in the design of SCP (Kim and Choi 2011, Liew *et al.* 2017, Yan *et al.* 2018).

The behavior of SCP has been extensively investigated through experiments and numerical analyses by many researchers (Oduyemi and Wright 1989, Qin *et al.* 2019, Roberts *et al.* 1996, Shanmugam *et al.* 2002, Yan *et al.* 2015, Yousefi and Ghalehnovi 2018, Zhang *et al.* 2014).

Shanmugam *et al.* (2002) studied the ultimate capacity of SCP with experiment and finite element analyses and showed the contribution of studs in the resisting capacity of SCP, Zhang *et al.* (2014) investigated the effect of studs on the level of composite action and development length of the steel plate in SCP. Yan *et al.* (2015) carried out experiments and numerical analyses to predict the influence of the steel plate on the ultimate strength of SCP. Furthermore, since Oduyemi and Wright (1989) suggested that the stable ratio of stud spacing to plate thickness is about 30, extensive research related to the stud spacing has also been performed. Roberts *et al.* (1996) carried out load tests on SCP subjected to bending and transverse shearing forces, and they showed that SCP is governed by yielding of the steel plate when the ratio of stud spacing to plate thickness is less than 40. Liang *et al.* (2004) established the elastic buckling coefficient to derive the buckling stress by using a finite element analysis, and Zhang *et al.* (2014) determined the maximum spacing to plate thickness ratio to prevent local buckling before yielding. Upon this background, further study on structural behavior of SCP is required since the allowable maximum stud spacing varies with the detailed geometric configuration, loading and boundary condition.

Generally, design codes and guidances such as the BS design code (BS5400 2005), Eurocode (Eurocode 4 2004), AISC design code (AISC 360 2010), AASHTO LRFD design code (AASHTO 2012) and DNV INCA guidance (Weitzenböck and Grafton 2010) have introduced regulations for the stud spacing to enhance the composite action between steel and concrete and to prevent local buckling in the steel plate. However, these regulations are very simple and conservative and hence there is some limitation in achieving more reasonable and efficient

*Corresponding author, Professor,
E-mail: khg@kaist.ac.kr

^a Ph.D. Student

^b Ph.D.

Table 1 Design codes and guidances for stud spacing

Design criteria	BS	Euro† code	AISC	AASHTO	DNV INCA Guidance
Stud spacing (s)	≤ 600 mm	$\geq 5d$	$\geq 6d$	$\geq 6d$	$\leq 0.75 \times (t_c + 2 \times t_s)$ (1)
	$\leq 3t_{slab}$	≤ 800 mm	$\leq 8t_{slab}$	≤ 600 mm	$\leq 22 \times t_s \times \sqrt{235/f_{yk-p}}$ (2)
	$\leq 4h$	$\leq 6t_{slab}$	≤ 900 mm		
Maximum stud spacing (s*)	564 mm	800 mm	900 mm	600 mm	150 mm (1) 94.35 mm (2)

* h = overall stud height (mm), t_{slab} = slab thickness by $t_c + 2t_s$ (mm), d = diameter of stud (mm),
 t_c = concrete thickness (mm), t_s = steel thickness (mm), f_{yk-p} = characteristic yield stress of steel plate (MPa),
 s^* = stud spacing calculated when $t_c = 188$ mm, $t_s = 6$ mm, $d = 13$ mm and $f_{yk-p} = 460$ MPa.

† In the Eurocode, if the slab is in contact over the full length with a steel compression flange, the Eq. (2) of the DNV INCA Guidance should be additionally considered

design. An improved design guideline to determine the stud spacing accordingly should be introduced. On the basis of numerous parametric studies to evaluate the relative influence of stud spacing on the stability of SCPs applied to the containment vessel subjected to biaxial normal stress, an improved ratio of the stud spacing to the thickness of the steel plate is proposed in this paper. design. An improved design guideline to determine the stud spacing accordingly should be introduced. On the basis of numerous parametric studies to evaluate the relative influence of stud spacing on the stability of SCPs applied to the containment vessel subjected to biaxial normal stress, an improved ratio of the stud spacing to the thickness of the steel plate is proposed in this paper.

2. Stability of SCP storage tank

2.1 Stud spacing in design codes

All design codes and design guidances describe the provision for the stud spacing. Table 1 shows the design criteria in the representative design codes that can be applied to the design of SCP. When the given criteria are satisfied, the steel plate will not develop local buckling before reaching the yielding state. Since the DNV INCA guidance is not only a design guidance specific to SCP structures but also gives the most conservative results, the final stud spacing is been usually determined from this guidance.

As shown in Table 1, INCA Guidance proposes two criteria, wherein Eqs. (1) and (2) are related to the shear cracking of an interior concrete block and the local buckling of steel plate, respectively, and generally Eq. (2) governs the stud spacing in the case of SCP used for storage tank structures. When a SCP storage tank is being constructed, concrete is poured within two steel skin plates, but the dense placement of steel studs makes the pouring of concrete difficult. Increasing the stud spacing is thus strongly required to facilitate pouring of concrete and to achieve design improvement in production cost and weight of the structure as well.

Upon this background, a review of Eq. (2) was first carried out. As shown in Eq. (2), the stud spacing s can be expressed by the relation $s = \alpha \cdot t_s \sqrt{235/f_{yk-p}}$. Elastic buckling analysis of a simply supported square plate

uniformly compressed in one direction produces the critical load of $\sigma_{cr} = 4\pi E_s / (12(1 - \nu^2)(s/t_s)^2)$ (Timoshenko and Gere 2009), and the prevention of buckling at the plate makes it possible to replace σ_{cr} with the yield strength f_y . Accordingly,

$s/t_s = \sqrt{4\pi E_s / 12(1 - \nu^2) f_y} = 56.8 \sqrt{235/f_y}$ (if the elastic modulus of steel $E_s = 210$ GPa and Poisson's ratio $\nu = 0.30$ are assumed), which means that the proportional constant α will be 56.8.

When a simply supported square plate with a span length of s is subjected to the action of uniformly distributed compressive forces in two perpendicular directions, the elastic stability analysis of the plate gives a decrease of the proportional constant down to $\alpha = 40.0$, and an additional change of the boundary condition from the simply supported to the pin-supported condition reduces the proportional constant to $\alpha = 24.0$. This means that Eq. (2) is conservative in determining the stud spacing because the determined spacing is smaller than that obtained from the pin-supported boundary condition which ignores the restraint for the deformation by the adjacent plates.

2.2 Elastic buckling analyses for stud spacing

To determine more reasonable stud spacing, accordingly, parametric studies were performed on the basis of an elastic buckling analysis. Since the experimental test of SCP modules subjected to bending and axial behaviors was executed (see 2.3 Experimental verification), the same dimensions and material properties as used in the experiment were taken for steel plate and the material properties that were used can be found in Table 2.

Fig. 1(a) represents the typical configuration for the exterior boundaries of SCP. Different from a small test specimen manufactured in a laboratory, a real-sized SCP will include channels along the exterior boundaries of the SCP to keep concrete within the skin plates during pouring, and these channels will introduce additional restraints for the deformation of the steel plate. Accordingly, two different boundary conditions are considered in additional parametric studies. As shown in Fig. 1(a), a total of 36 bare steel panels are considered in the modeling and two different boundary conditions of (1) pin-supported by studs only and (2) pin-supported by studs at the interior supports and simply supported by channels along the four exterior

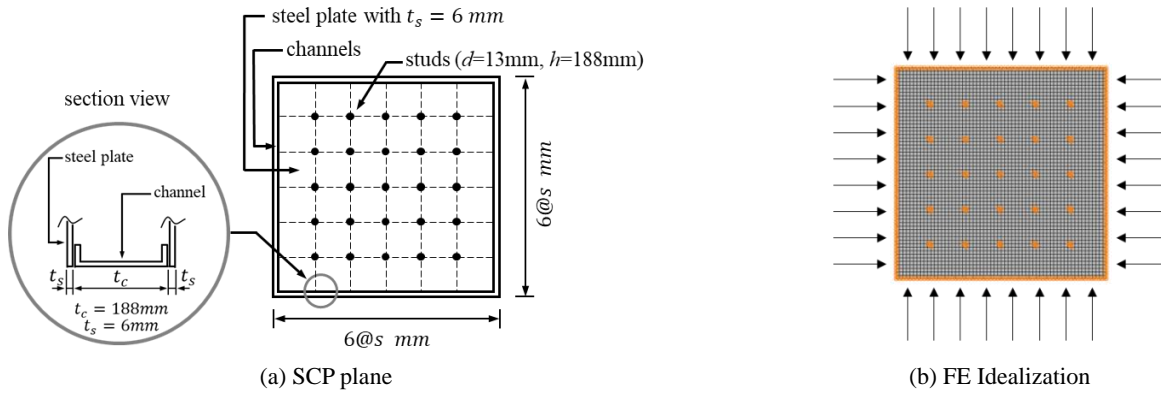


Fig. 1 Geometric configuration of steel plate with channels

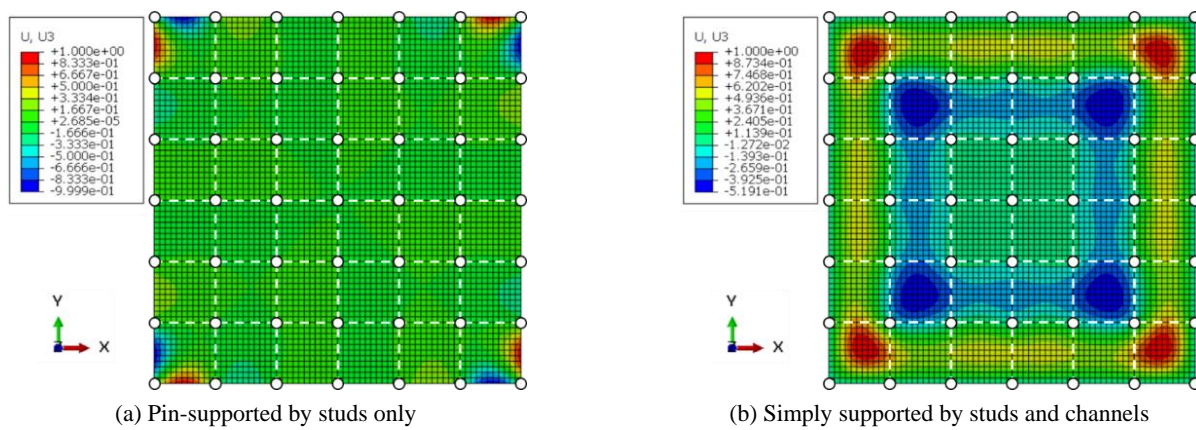


Fig. 2 Deformation in steel plates

boundaries are considered. Fig. 1(b) shows the corresponding finite element idealization of the exterior steel plate.

Fig. 2 shows the vertical deformation at the critical loading stage in the bared steel plate with $s = 165$ mm subjected to biaxial normal pressure, and it can be considered as equivalent to the buckling mode. While the stud supports along the exterior boundaries produce a critical stress condition at the most exterior boundaries, the addition of channels at the four exterior boundaries moves the critical position to the interior panels (see Fig. 2). On the basis of additional parametric studies with change of the stud spacing, the optimum stud spacing that gives the equivalence between the yielding load and the critical load of plates can be determined, and the obtained space was $s = 133$ mm for the elastic steel plates supported by studs only and $s = 168$ mm for the studs and channels supported steel plates, respectively, as shown in Fig. 3.

The obtained results represent that the stud spacing determined from the design codes (see Table 1), especially by the DNV INCA Guidance ($s \leq 94.3$ mm), gives conservative results, and the installation of channels that are used as permanent formworks to prevent concrete spilled out of form while pouring concrete introduces an increase in the buckling strength of steel plates with a 26% increase in the stud spacing. In conclusion, the current regulations related to the stud spacing is too conservative to directly

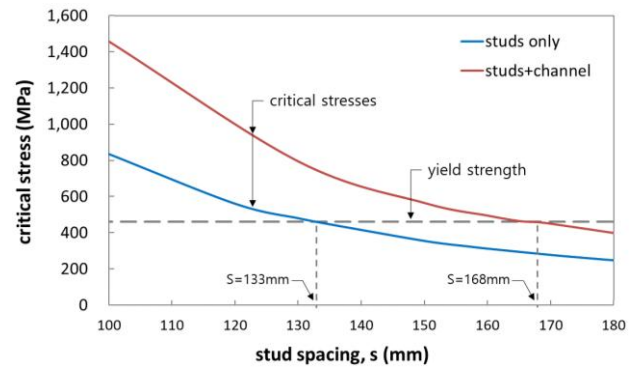


Fig. 3 Critical stresses with the change in the stud spacing

apply to SCP members, and a more reasonable design criterion for the stud spacing of SCP members should be suggested upon consideration of the manufacturing of SCP.

2.3 Experimental verification

Since the design criterion for the stud spacing must be based on many parametric studies, numerical and experimental verifications of the used numerical model that we have employed must be conducted to reserve reliability of the obtained numerical results. The composition of SCP members demands consideration of the bond-slip effect

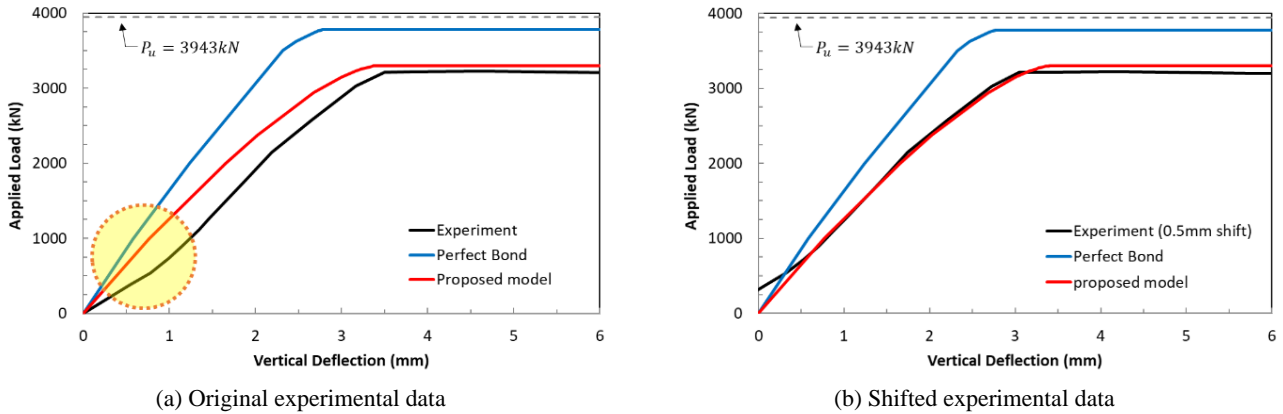
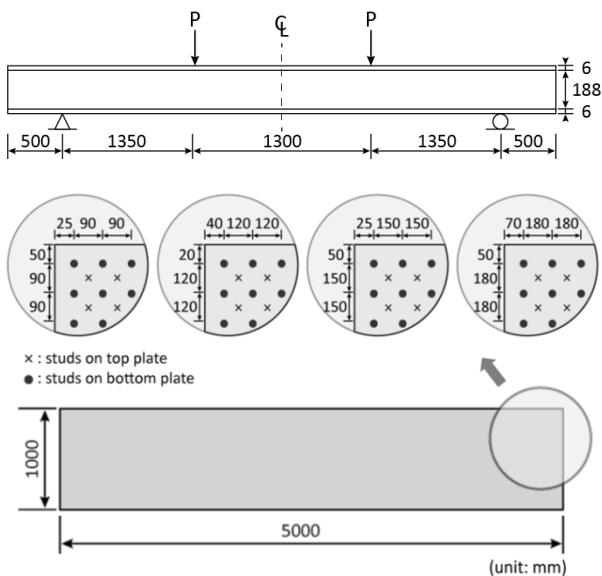


Fig. 6 Load-deflection relation of compressive strength test



(a) Experimental setup



(b) Geometric configuration

Fig. 7 Compressive strength test of SCP

of sliding in the experimental setup due to the discordance between the loading axis and the specimen axis. Therefore, the experimental data have been shifted and then compared with the numerical results in Fig. 6(b).

As shown in Fig. 6(b), relatively close agreement between the analyses and experiment was obtained in predicting the ultimate resisting capacity of the specimen, and the evaluated deformation history up to the maximum axial force is almost coincident with that obtained from the experiment. On the other hand, the numerical results obtained by the perfect bond assumption overestimate the ultimate load and converge to the ultimate compressive force determined by $P_u = f_c A_c + 2f_y A_s = 3,943 \text{ kN}$,

which is larger than the nominal compressive strength of $P_n = 3,662 \text{ kN}$ evaluated from the KEPIC-SNG design guideline (KEPIC-SNG 2010). This means that the bond-slip effect is dominant at the SCP member subjected to axial force and must be taken into consideration to exactly predict the maximum axial force. In advance, the proposed numerical model with the use of the equivalent modulus of elasticity in steel only can effectively consider the bond-slip effect, without taking double nodes which complicate the numerical modeling.

Additional correlation studies between experiments and analytical results were conducted on the flexural test specimens. Fig. 7 illustrates the experimental setup and the corresponding geometric configuration of the specimens. Since the maximum stud spacing determined through the elastic stability analyses for SCP panels simply supported by studs was only 150 mm, three specimens with different stud spacing of 120 mm, 150 mm, and 180 mm were tested and the obtained data were compared with the analytical results.

Fig. 8 presents a comparison of the experimental data with analytically predicted results for the midspan deflection. As shown in this figure, the obtained results lead to almost the same conclusions as those mentioned in the case of the compressive strength test. The consideration of the bond-slip effect is very important in predicting the ultimate bending capacity of SCP members and the proposed analytical approach can effectively be used.

In particular, different from the first three cases, the last case with a stud spacing of 180 mm presents a slight decrease of the resisting capacity and an increase of the midspan deflection. This appears to be caused by the occurrence of local buckling at the exterior steel plate on the top face of the specimen. Nevertheless, although the ultimate resisting capacity slightly decreased, the structural behavior was stable until reaching the ultimate resisting capacity of the specimen because the stud spacing of 180 mm is not far beyond the limiting value. Accordingly, on the basis of both correlation studies, it can be concluded that the numerical approach considering the bond-slip effect with the proposed model can be used to determine the ultimate resisting capacity of SCP members.

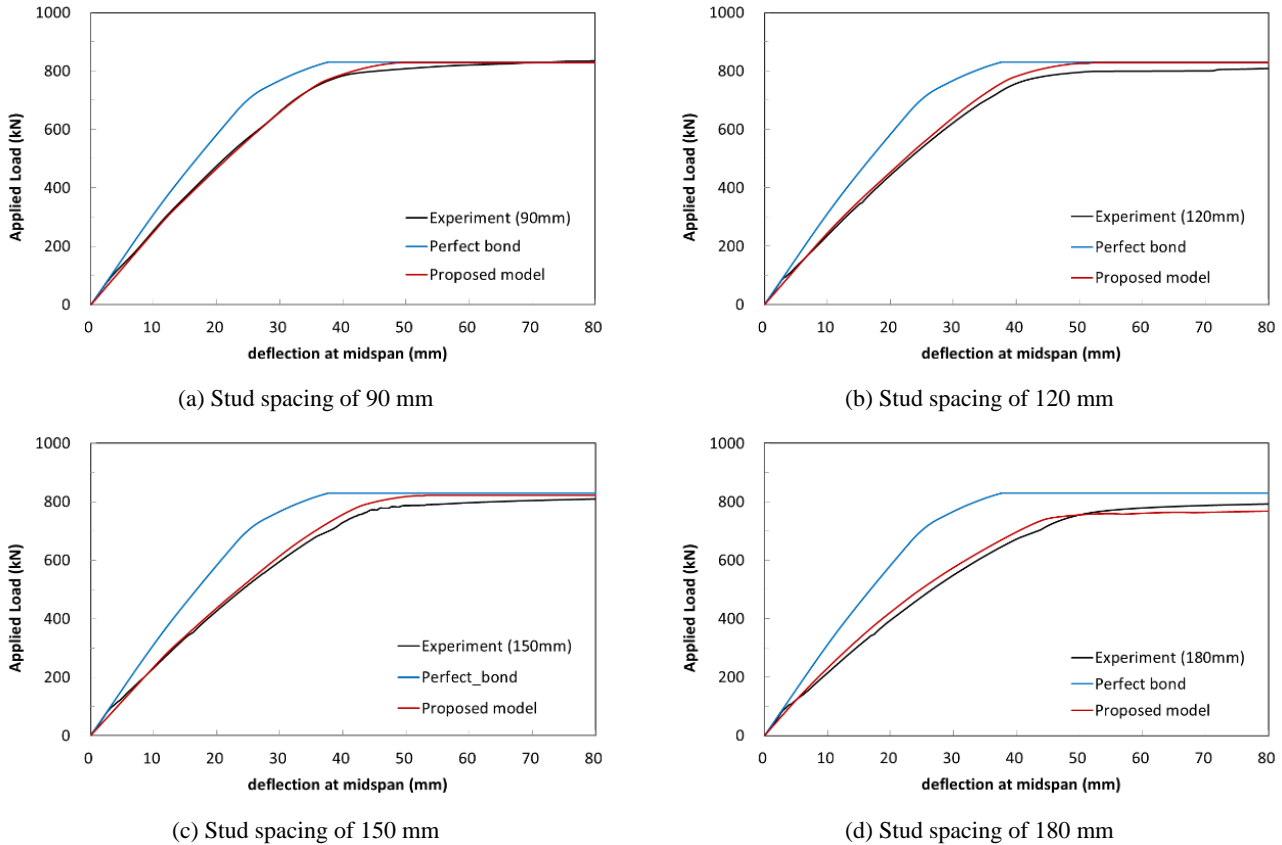


Fig. 8 Load-deflection relation of flexural strength test

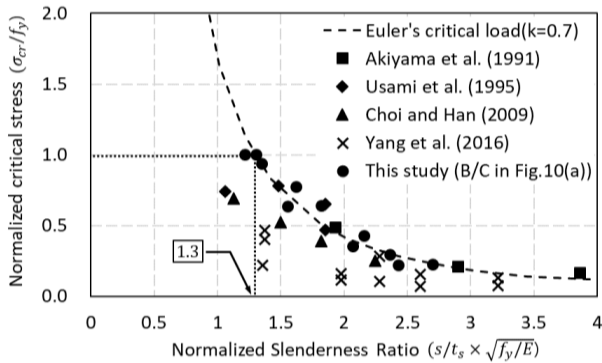


Fig. 9 Comparison of numerical results with the experimental datad

3. Parametric studies for stud spacing

In addition to the stability analyses of bare steel plates in Fig. 2, experiments for SCP members have also been carried out by many researchers (Akiyama *et al.* 1991, Choi and Han 2009, Kanchi 1996, Usami *et al.* 1995, Yang *et al.* 2016). More than forty SCP members with the stud spacing to plate thickness ratio (s/t_s) ranging from 20 to 50 were tested and Zhang *et al.* (2014) suggested using the Euler's column buckling curve with an effective length coefficient k equal to 0.7 to represent the critical stress of SCP panels, $\sigma_{cr} = \pi^2 E_s / (12k^2 (s/t_s)^2) = 1.6785 E_s / (s/t_s)^2$. In advance, the critical buckling stress gives a limiting ratio

of $s/t_s = 1.3 \sqrt{E_s/f_y}$ when $\sigma_{cr} = f_y$ and produces the proportional constant of $\alpha = 38.86$ in the expression for the stud spacing of $s = \alpha \cdot t_s \sqrt{235/f_y}$ (see Fig. 9). This means that the channels installed in the specimens to keep concrete within both skin plates while pouring concrete develops a restraint effect equivalent to the simply supported boundary condition.

However, the accuracy of the critical stress may depend on the exactness of the test setup. Because of the initial imperfection of the specimen, the bond-slip along the steel-concrete interface and the instability of the boundary condition, the experimentally determined buckling stress has been decreased and a few researchers (Cho *et al.* 2014, Zhang *et al.* 2014) proposed the critical s/t_s ratio as $s/t_s = 1.0 \sqrt{E_s/f_y}$, which corresponds to $k = 0.91$ and $\alpha = 29.89$.

Upon this background, elastic stability analyses were performed to investigate the maximum stud spacing influenced by the channel, which is placed along the end face of the skin plates (see Fig. 10). Three different boundary conditions that describe the connection situations between the adjacent SCP members were considered as shown in Fig. 10. Here the simply supported boundary condition (Fig. 10(a)) means restraint for the displacement in the z -direction along the end faces of the SCP member, and uncovering (Fig. 10(b)) and covering (Fig. 10(c)) conditions of the stud represent additional placement of a channel with a flange shorter and longer than the distance to

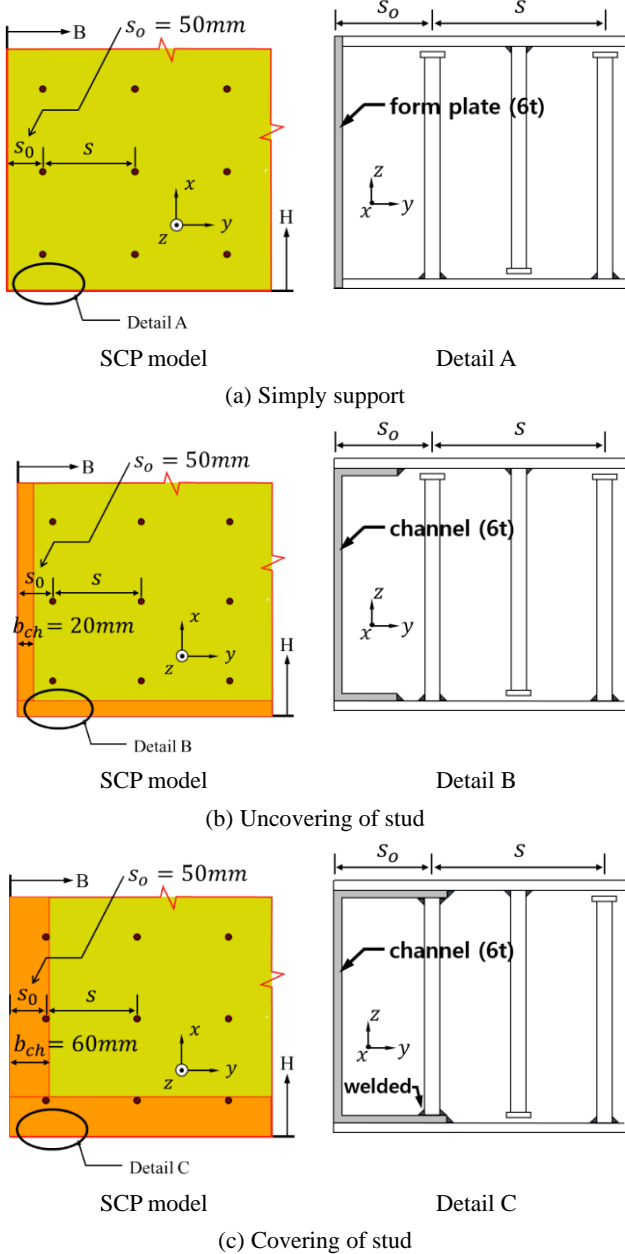


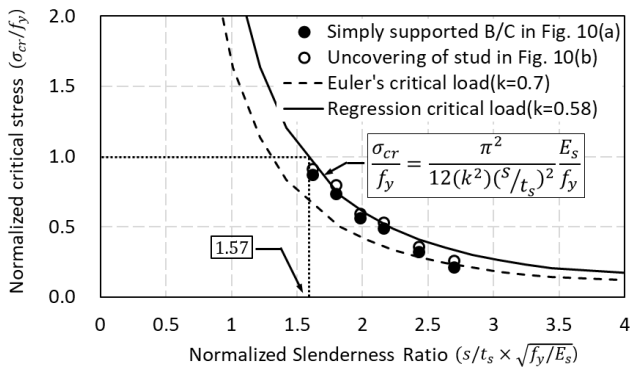
Fig. 10 Boundary condition and corresponding channel placement in SCP members

the first steel stud arrangement along the end faces of the SCP member, respectively.

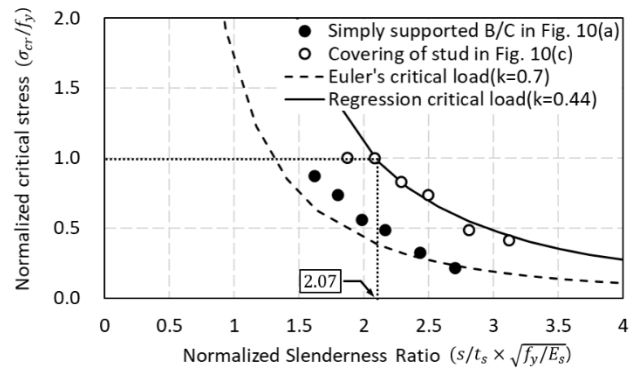
SCP members with $B \times H = 12 \text{ m} \times 3 \text{ m}$ and the thickness of the steel plate $t_s = 4.5 \text{ mm}$ and 6.0 mm were considered. The thickness of interior concrete and the diameter of steel stud d_s were assumed to be 280 mm and 10 mm , respectively. The distance s_0 from the outermost edge to the stud was 50 mm in all cases and the width of the channel b_{ch} was 20 mm and 60 mm for case B and case C, respectively. Since the critical load is related to the stability of the skin plate, axial compressive forces were applied directly to the skin plate. The bond-slip effect was taken into consideration and the FE mesh discretization of each constituent component was determined through a convergence test of the FE mesh size.

The numerical results obtained for the simply supported steel plate in Fig. 10(a) subjected to uniaxial compressive force are incorporated in Fig. 9 and they show that the critical stresses trace Euler's column buckling curve with an effective length coefficient $k = 0.7$ quite closely, although they seem to correspond with the upper bound values of the experimental data. This indicates that the critical stress depends on the boundary condition along the end face of the skin plate, regardless of the thickness and size of the steel plate. It further shows that the bond-slip effect does not dominantly affect the value of the critical stress, although it causes additional deformation of SCP members, because the structural response is dominantly affected by the stability of the steel plate with an increase of the slenderness ratio.

The change in the boundary condition through the addition of a steel channel along the end face of the skin plate may produce an increase of the rotational stiffness, which in turn induces an increase of the critical stress. As shown in Fig. 11(a), the addition of channels along the end face of the skin plate yields difference in the obtained results relative to those for the simply supported boundary condition in Fig. 10(a). In addition, the extension of the channel height to the outmost steel studs causes a remarkable increase of the critical stress. Adoption of the boundary condition in Fig. 10(c) makes it possible to enlarge the stud spacing. That is, the stud spacing has been extended from $s \leq 1.57t_s\sqrt{E_s/f_y}$ to $s \leq 2.07t_s\sqrt{E_s/f_y}$. Accordingly, the stud spacing mentioned in the DNV INCA



(a) Uncovering of stud



(b) Covering of stud

Fig. 11 Buckling behaviors in channeled SCP under uniaxial loading

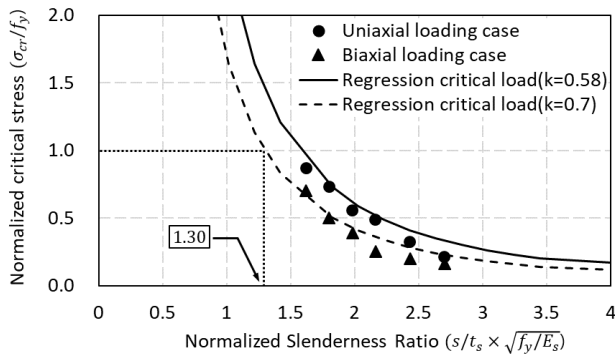


Fig. 12 Buckling behaviors in simply supported SCP

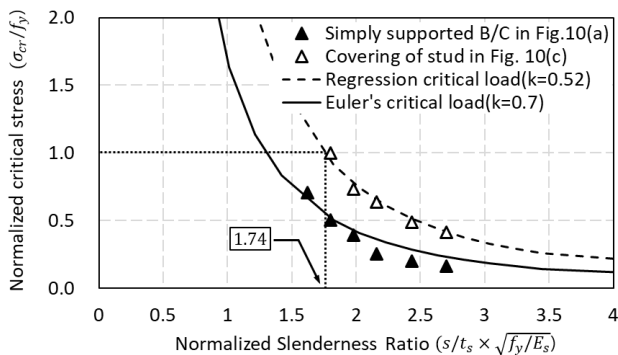


Fig. 13 Buckling behaviors in SCP under biaxial loading

guidance ($\alpha = 22$) can be increased up to 281% corresponding to a proportional constant of $\alpha = 61.88$ and an increase of the stud spacing will greatly facilitate pouring of concrete while fabricating a SCP member.

A few structures including on-ground LNG tanks and general storage tanks may be subjected to biaxial loading or triaxial loading conditions. To consider the change in the structural behavior according to the loading condition, the same SCP members were analyzed under biaxial loading (see Fig. 1(b)), and the obtained results can be found in Figs. 12 and 13. The biaxial loading causes about an 18% decrease of the critical stress and the stud spacing. In case of the boundary condition in Fig. 10(b), the stud spacing has been decreased from $s \leq 1.57t_s\sqrt{E_s/f_y}$ to $s \leq 1.30t_s\sqrt{E_s/f_y}$ by the application of biaxial loading. Nevertheless, this reduced stud spacing still corresponds to the proportional constant $\alpha = 38.86$, and the members subjected to biaxial loading will be limited at dome structures in the containment structures. In particular, the placement of a steel stud within the height of the end channel (boundary condition in Fig. 10(c)) results in an increase of the stud spacing from $s \leq 1.30t_s\sqrt{E_s/f_y}$ to $s \leq 1.74t_s\sqrt{E_s/f_y}$ (see Figs. 12 and 13), while producing a proportional constant of $\alpha = 52.01$. It can be suggested, accordingly, that the proportional constant of α can be increased at least to $\alpha = 33.0$ in design practice, which is equivalent to $s \leq 1.10t_s\sqrt{E_s/f_y}$, considering the construction situation for pouring concrete in a SCP member. This value of $\alpha = 33.0$ also satisfies the other

limiting value in Eq. (1) related to the shear resistance. Especially since the shear design criterion is not considered in this paper, the proposed value of α must be less than the limiting value determined from Eq. (1).

4. Conclusions

One of the key issues in the design and construction of SCP members is to determine a reasonable shear stud spacing, because the shear stud provides composite action between exterior steel faceplates and the interior concrete matrix and prevents local buckling of the steel plate before yielding as well. Since current design codes produce very conservative results in the stud spacing, this paper introduces an improved guideline for the stud spacing through parametric studies for SCP subjected to the uniaxial and/or biaxial compressive forces.

The obtained numerical results show that the proportional constant $\alpha = s/t_s\sqrt{f_y/E_s}$ can be increased at least to $\alpha = 33.0$ from $\alpha = 22.0$ considered in the current design practice. In advance, the placement of the outmost steel studs within the channel height will increase the value of the proportional constant up to $\alpha = 61.88$, which gives 281% larger stud spacing than the current reference. This means that an increase of the stud spacing with placement of the outmost stud within the channel height should be considered for more rational design and placement of the steel shear studs.

Acknowledgments

This work is supported by the Korea Agency for Infrastructure Technology Advancement(KAIA) grant funded by the Ministry of Land, Infrastructure and Transport (Grant 13IFIP-C113546-01).

References

- AASHTO (2012), AASHTO LRFD bridge design specifications, American Association of State Highway and Transportation Officials, Washington, D.C., USA.
- AISC 360 (2010), Specification for structural steel buildings, American Institute of Steel Construction; Chicago, IL, USA.
- Akiyama, H., Sekimoto, H., Fukihara, M., Nakanishi, K. and Hara, K. (1991), "A compression and shear loading tests of concrete filled steel bearing wall", *Transactions of the 11th Structural Mechanics in Reactor Technology*, 323-328.
- BS5400 (2005), Steel, concrete and composite bridges, Part 5, Code of practice for the design of composite bridges. British Standard Institution, London, UK
- Cho, S.-G., Lim, J.-S., Jeong, Y.-D., and Yi, S.-T. (2014), "Analytical Study for Design of Shape and Arrangement Spacing of Studs in Steel Plate Concrete(SC) Wall subjected to Shear and Axial Forces", *J. Korea Inst. Struct. Mainten. Inspec.*, **18**(4), 67-76. <https://doi.org/10.11112/jksmi.2014.18.4.067>
- Choi, B.J. and Han, H.S. (2009), "An experiment on compressive profile of the unstiffened steel plate-concrete structures under compression loading", *Steel Compos. Struct., Int. J.*, **9**(6), 519-534. <https://doi.org/10.12989/scs.2009.9.6.519>
- Eurocode 4 (2004), Design of composite steel and concrete

- structures Part 1-1 : General rules and rules for buildings. European Committee for Standardization; Brussels, Belgium.
- Hwang, J.W. and Kwak, H.G. (2013), "Improved FE model to simulate interfacial bond-slip behavior in composite beams under cyclic loadings", *Comput. Struct.*, **125**, 164-176. <https://doi.org/10.1016/j.compstruc.2013.04.020>
- Kanchi, M. (1996), "Experimental study on a concrete filled steel structure Part. 2 Compressive Tests (1)", *Summary of Technical Papers of Annual Meeting, Architectural Institute of Japan, Structures*, pp. 1071-1072.
- KEPIC-SNG (2010), Specification for safety-related steel plate concrete structures for nuclear facilities, Korea Electric Association, Seoul, Republic of Korea.
- Kim, W.B. and Choi, B.J. (2011), "Shear strength of connections between open and closed steel-concrete composite sandwich structures", *Steel Compos. Struct., Int. J.*, **11**(2), 169-181. <https://doi.org/10.12989/scs.2011.11.2.169>
- Kwak, H.G. and Hwang, J.W. (2010), "FE model to simulate bond-slip behavior in composite concrete beam bridges", *Comput. Struct.*, **88**(17-18), 973-984. <https://doi.org/10.1016/j.compstruc.2010.05.005>
- Lee, W.H., Kwak, H.G. and Hwang, J.Y. (2019), "Bond-slip Effect in Steel-Concrete Composite Flexural Members: (1) Simplified Numerical Model", *Steel Compos. Struct., Int. J.*, **32**(4), 537-548. <https://doi.org/10.12989/scs.2019.32.4.537>
- Liang, Q.Q., Uy, B., Wright, H.D. and Bradford, M.A. (2004), "Local buckling of steel plates in double skin composite panels under biaxial compression and shear", *J. Struct. Eng.*, **130**(3), 443-451. [https://doi.org/10.1061/\(ASCE\)0733-9445\(2004\)130:3\(443\)](https://doi.org/10.1061/(ASCE)0733-9445(2004)130:3(443))
- Liew, J.R., Yan, J.B. and Huang, Z.Y. (2017), "Steel-concrete-steel sandwich composite structures-recent innovations", *J. Constr. Steel Res.*, **130**, 202-221. <https://doi.org/10.1016/j.jcsr.2016.12.007>
- Oduyemi, T.O.S. and Wright, H.D. (1989), "An experimental investigation into the behaviour of double-skin sandwich beams", *J. Constr. Steel Res.*, **14**(3), 197-220. [https://doi.org/10.1016/0143-974X\(89\)90073-4](https://doi.org/10.1016/0143-974X(89)90073-4)
- Oehlers, D.J. and Bradford, M.A. (1999), *Elementary behaviour of composite steel and concrete structural members*, Butterworth-Heinemann.
- Qin, Y., Li, Y.-W., Lan, X.-Z., Su, Y.-S., Wang, X.-Y. and Wu, Y.-D. (2019), "Structural behavior of the stiffened double-skin profiled composite walls under compression", *Steel Compos. Struct., Int. J.*, **31**(1), 1-12. <https://doi.org/10.12989/scs.2019.31.1.001>
- Roberts, T.M., Edwards, D.N. and Narayanan, R. (1996), "Testing and analysis of steel-concrete-steel sandwich beams", *J. Constr. Steel Res.*, **38**(3), 257-279. [https://doi.org/10.1016/0143-974X\(96\)00022-3](https://doi.org/10.1016/0143-974X(96)00022-3)
- Shanmugam, N.E., Kumar, G. and Thevendran, V. (2002), "Finite element modelling of double skin composite slabs", *Finite Elem. Anal. Des.*, **38**(7), 579-599. [https://doi.org/10.1016/S0168-874X\(01\)00093-2](https://doi.org/10.1016/S0168-874X(01)00093-2)
- Simulia, D. (2017), Abaqus 6.17 Documentation, DS SIMULIA Corp., USA.
- Timoshenko, S.P. and Gere, J.M. (2009), *Theory of Elastic Stability*, Courier Corporation, MA, USA.
- Usami, S., Hara, K., Sasaki, N., Akiyama, H., Narikawa, M. and Takeuchi, M. (1995), "Study on a concrete filled steel structure for nuclear power plants (part 2). Compressive loading tests on wall members", *Transactions of the 13. International Conference on Structural Mechanics in Reactor Technology*. v. 4.
- Weitzenböck, J.R. and Grafton, T. (2010), "Assessment of the INCA steel-concrete-steel sandwich technology—a public report", DNV, Det Norske Veritas, NO-1322, Høvik, Norway.
- Yan, J.B., Liew, J.R., Zhang, M.H. and Soheli, K.M.A. (2015), "Experimental and analytical study on ultimate strength behavior of steel-concrete-steel sandwich composite beam structures", *Mater. Struct.*, **48**(5), 1523-1544. <https://doi.org/10.1617/s11527-014-0252-4>
- Yan, J.-B., Wang, Z., Wang, T. and Wang, X.-T. (2018), "Shear and tensile behaviors of headed stud connectors in double skin composite shear wall", *Steel Compos. Struct., Int. J.*, **26**(6), 759-769. <https://doi.org/10.12989/scs.2018.26.6.759>
- Yang, Y., Liu, J. and Fan, J. (2016), "Buckling behavior of double-skin composite walls: An experimental and modeling study", *J. Constr. Steel Res.*, **121**, 126-135. <https://doi.org/10.1016/j.jcsr.2016.01.019>
- Yousefi, M. and Ghalehnavi, M. (2018), "Finite element model for interlayer behavior of double skin steel-concrete-steel sandwich structure with corrugated-strip shear connectors", *Steel Compos. Struct., Int. J.*, **27**(1), 123-133. <https://doi.org/10.12989/scs.2018.27.1.123>
- Zhang, K., Varma, A.H., Malushte, S.R. and Gallocher, S. (2014), "Effect of shear connectors on local buckling and composite action in steel concrete composite walls", *Nuclear Eng. Des.*, **269**, 231-239. <https://doi.org/10.1016/j.nucengdes.2013.08.035>

CC